Study of the rejection of contaminants of emerging concern by a biomimetic aquaporin hollow fiber forward osmosis membrane

Mónica Salamanca[1,3*], Rebeca López-Serna[1,3], L. Palacio[1,2], A. Hernandez[1,2], P. Prádanos[1,2], Mar Peña[1,3]

1. Institute of Sustainable Processes (ISP), Dr. Mergelina s/n, 47011, Valladolid, Spain.
2. Surfaces and Porous Materials (SMAP), Associated Research Unit to CSIC. University of Valladolid, Facultad de Ciencias, Paseo Belén 7, E-47011 Valladolid, Spain.
3. Department of Chemical Engineering and Environmental Technology, Dr. Mergelina s/n, 47011 Valladolid, Spain

* Corresponding author: e-mail address: monica.salamanca@uva.es

Abstract

Forward osmosis (FO) plays an increasingly important role in membrane processes because of its advantages compared to traditional pressure-driven membrane processes. There are different types of water-selective FO membranes. In this study, a biomimetic hollow fiber module comprising an active layer of polyamide thin film composite (TFC) with integrated aquaporin proteins and an effective area of 0.6 m^2 is used to study the rejection of 24 Contaminants of Emerging Concern (CECs). The rejections obtained for all the contaminants studied were higher than 93% and for 19 of them rejections of up to 99% were reached. It was observed that although all the tested compounds showed rejections very close to 100 %, they were not completely recovered in the feed solution which makes the retention within the membrane an important factor to be considered. Hence, two membrane rinses were necessary after each membrane operation to completely recover each contaminant. The results were analyzed considering the

physicochemical properties (molecular weight, charge and hydrophobicity) of the contaminants.

Keywords: Forward Osmosis (FO); Aquaporin membrane; Contaminants of Emerging Concern (CECs); Hollow fiber module.

1. Introduction

In recent decades, there has been a growing interest in Contaminants of Emerging Concern (CECs). They are organic pollutants that are present in the environment at increasingly abundant concentrations, as detected in current studies, and can cause damage to the environment and human health [1–3]. Only recently, some of these compounds have been included in the environmental legislation as they were previously not easily detected due to the lack of robust enough analysis technologies. Nevertheless, thanks to new methodologies and alarming research on their effects, concentrations limits are beginning to be considered and established [4–9].

The main sources of emerging contaminants include pesticides used in agriculture, veterinary drugs and food additives used in livestock farming, Pharmaceuticals and Personal Care Products (PPCPs) which, if not fully metabolized in the body, can be excreted through urine and feces, reaching Waste Water Treatment Plants (WWTP) and eventually arriving to the water bodies. All these sources can cause point source pollution, but also diffuse pollution by leaching into surface waters and groundwater as a result of rainfall, soil infiltration and surface runoff. One of the most important problems for the aquatic environment is the discharge of effluents from hospitals, industrial and the urban WWTPs [10–12]. The presence of CECs in the water

environment is known to potentially affect aquatic organisms and result in changes that threaten the sustainability of aquatic ecosystems. Although some contaminants can be efficiently removed in WWTPs, the removal of CECs is often insufficient. CECs are detected in both influents and effluents ranging from ng/L to mg/L [1,2,13,14]. Conventional WWTPs are not specially designed to remove these pollutants, and therefore many of these compounds appear in their effluents. Consequently, its introduction into surface water and subsequently into drinking water exposes us to such substances and their possible effects.

There are advanced oxidation technologies that can eliminate some of these microcontaminants from residual waters like Activated Carbon (AC), ozonation, UltraViolet (UV) irradiation, sonodegradation and also Membrane BioReactors (MBR) and membrane filtration processes. [15–20].

Pressure-driven membrane techniques such as NanoFiltration (NF) and Reverse Osmosis (RO) have also been used to treat microcontaminant-contaminated water. NF has been found to be efficient for some large contaminants while RO effectively removes small contaminants. However, due to high hydraulic pressures and concentration polarization, RO has several disadvantages, such as membrane fouling, increased costs, and scale limitations [21].

A possible alternative to overcome RO and NF drawbacks could be the use of the Forward Osmosis (FO) processes [22]. In the forward osmosis process, the driving force is the osmotic gradient instead of pressure driven force, which could be an important advantage about membrane fouling. In this process, the osmotic pressure gradient between a concentrated extraction solution and a less concentrated feed solution is used to facilitate the transport of water through a semipermeable membrane, allowing water

molecules to pass while retaining other solutes. This leads to dilution of the draw solution, while the solutes in the feed stream are being concentrated [23,24]. This process does not apply hydraulic pressure, resulting in a lower propensity for irreversible fouling of the membrane and lower energy cost compared to NF / RO processes. However, FO is a technology that requires more study since although the membrane fouling is quite low, the permeate fluxes are also not very high and this is a limitation in scaling [22].

There are different types of forward osmosis membranes that have been studied in the rejection of pollutants in recent years such as Cellulose TriAcetate (CTA) membranes, for which a wide range of data are available on their rejection characteristics for different trace organic compounds [25–29]. Hancock et al. (2011) shown that CTA membranes had a high rejection towards different organic traces when tested on a pilot scale, whereas when it was done on a bench scale, the membrane rejection capabilities decreased [30].

Furthermore, a comparative study between a CTA membrane and a Thin Film Composite (TFC) FO membrane showed advantages of the TFC membrane with respect to water permeability, rejection of organic traces and pH stability [31].

Frequently plate and frame or spiral bound modules are used. Nevertheless, for applications that require light weight and low space designs (eg, portable FO systems), as well as large volume separations, other membrane configurations, such as Hollow Fiber (HF) modules, may be advantageous. Promising, and commercially available in hollow fiber modules, are those integrating Aquaporin proteins. They are transmembrane proteins mainly promoting water permeation, which are attached within the active layer of the membrane [32,33]. The Aquaporin membranes include aquaporin

proteins that give a high-water transport in a very selective way with high chemical resistance including resistance bearing cleaning procedures with all the customary chemical agents [34].

Substantial improvements in water permeability have been fully demonstrated in the literature reaching 5 to 1000 times bigger permeabilities [34,35].

Engelhardt et al. (2018) tested a hollow fiber Aquaporin membrane model to reject three Trace Organic Contaminants (TrOCs). They reported> 99% rejection for all tested compounds [36]. Nikbakht et al. (2020) studied the rejection of three pesticides with an Aquaporin hollow fiber membrane and compared the results with those obtained with a flat sheet FO membrane. They reported >98% rejection for the three pesticides with the HF membrane [37]. In this study, through preliminary evaluation, it was shown that using a small, low-cost FO configuration could be scaled by a laboratory scale FO configuration or a small pilot scale configuration due to reproducibility of results.

So far, few research groups have investigated the potential of Aquaporin hollow fiber membranes in removing emerging contaminants. Up to now, mostly flat sheet membranes have been used for this purpose. There are still few studies carried out with forward osmosis technology, and many emerging compounds present in the environment. In this respect and taking into account this background the objective of this work is to study the behavior of a hollow fiber Aquaporin membrane to evaluate the rejection of a total of 24 emerging contaminants from different groups such as Antibiotics (Ciprofloxacin, Ofloxacin, Sulfamethoxazole, Metronidazole, Erythromycin, Clarithromycin), Analgesics (Diclofenac, Naproxen, Ibuprofen, Salicylic acid, Acetaminophen), Lipid regulators (Clofibric acid, Gemfibrozil), Psychiatric drugs (Carbamazepine), Antimicrobials (Triclosan), Hormones (17-α -

Ethinylestradiol (EE2), 17-β-Estradiol (E2), Estrone (E1)), β-blocker (Atenolol), X-ray contrast (Iohexol), Stimulant (Caffeine), Anti-itching (Crotamiton) Insect repellant, (DEET) and Herbicides (Atrazine). In addition, changes in membrane flow, different Draw Solution (DS) concentrations, and different doping concentrations of some of the contaminants were investigated to better understand the membrane behavior.

2. Materials and Methods

2.1. Experimental setup

The FO concentration system (Fig. 1) consisted of a membrane module provided with a feed solution (FS) and a draw solution (DS) compartments. An Aquaporin Inside^{TM} FO hollow fiber module (Aquaporin A/S, Kongens-Lingby, Denmark) was used for the experiments. The hollow fiber module contains 0.6 m^2 of a membrane with an active layer of thin film composite (TFC) polyamide with integrated aquaporin proteins. Counter-current recirculation closed circuits of the feed and draw solutions were applied on each side of the FO membrane via two peristaltic pumps. In all experiments FS was pumped through the lumen side of the hollow fibers (active side) while the DS was pumped through the shell side. The feeding container starts from 2L of MilliQ water with magnetic stirring and the extraction solution container with 1L of NaCl. The device has been operated with different NaCl concentration and flow rates. All changes in volume of DS were measured by weighing using digital electronic scales to calculate the water flux. Moreover, a conductivity meter was immersed in both solutions to measure concentration and to evaluate the saline flux. To know the FS and DS flow rates through the corresponding loops and the inlet and outlet pressures, two flowmeters and two manometers were placed, as shown in figure 1. It is worth noting that any

147 pretreatment, totally essential for real WWTPs effluents, should be needed in our
148 conditions.

149

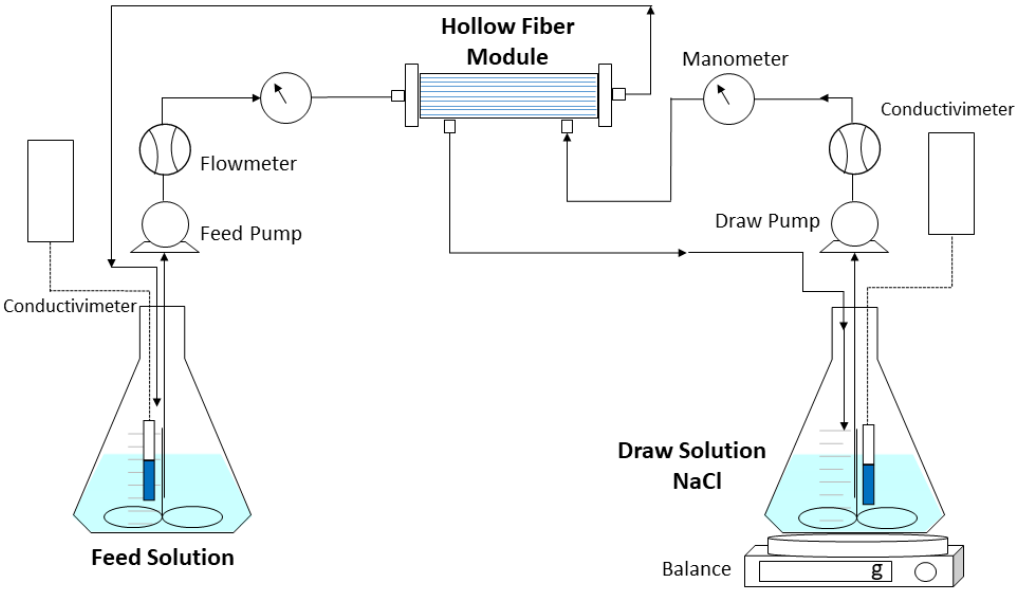

Figure 1. Schematic illustration of the FO setup.

150

151 Membrane specifications can be found in Table 1. These membranes have a dense active
152 layer inside the fiber with a porous Support layer on the external side of the fiber. They
153 consist of a biomimetic TFC selective layer [38] supported by polysulfone fibers. SEM
154 pictures of flat and hollow fiber aquaporin membranes can be found in the literature [34,
155 39, 40]. Fini et al. [37] made a revision of literature on contact angles for Aquaporin flat
156 membranes registering results from 59º to 96º with an average value of 73º. This contact
157 corresponds to a fairly high hydrophilicity for the aquaporin flat membrane that could be,
158 without risk, assumed for our hollow fiber membranes.

159

160 **Table 1**. Specifications for the Aquaporin Inside ™ FO hollow fiber module as

161 provided by the membrane manufacturer.

Manufacturer	Aquaporin A/S (Copenhagen, Denmark)
Membrane module	HFFO.6
Active area	0.6 m^2
Number of fibers	8000
Fiber length	120 mm
Inner diameter of fibers	200 μm
Wall thickness of fiber	35 μm
Active layer	Polyamide thin film composite (TFC) with AQP vesicles
Porous support layer	Polysulfone (PS)
Cross sectional area shell	3.28E-05 m^2
Cross sectional area lumen	2.51E-04 m^2
Water flux (DI water vs.0.5M NaCl, 25 L/h as feed flow rate and 15 L/h as draw flow rate, temperature 298 K)	11 ± 1.5 L/m^2h
Specific reverse salt flux (DI water vs.0.5M NaCl, 25 L/h as feed flow rate and 15 L/h as draw flow rate, temperature 298 K)	0.15 ± 0.05 g/L

162

163 *2.2. Membrane characterization and operation conditions*

164 To characterize the initial membrane operation, the tests recommended by the

165 manufacturer have been carried out. These tests have been also carried out before each

166 experiment, to check membrane performance, with the different emerging contaminants

167 assayed.

168 To determine the reverse salt flux, J_s and the water flux J_w , weight and conductivity

169 measurements were taken every minute for the duration of the experiment, and both

170 volume and salt flows are extrapolated to zero time.

171 To calculate J_s , equation (1) was used, where $C_{FS\,t_{i+1}}$ is the salt concentration of the

172 feed solution in time t_{i+1} , $C_{FS\,t_i}$ the salt concentration of the feed in time t_i , $V_{FS\,t_{i+1}}$ and

173 $V_{FS\,t_i}$ are the feed volumes in times t_{i+1} and t_i respectively and A is the surface area

174 of the active side of the membrane.

175 $$J_S = \frac{C_{FS\,t_{i+1}} V_{FS\,t_{i+1}} - C_{FS\,t_i} V_{FS\,t_i}}{A(t_{i+1} - t_i)} \quad (1)$$

176 J_w was calculates by using equation (2).

177 $$J_w = \frac{V_{FS\,t_{i+1}} - V_{FS\,t_i}}{A(t_{i+1} - t_i)} \quad (2)$$

178 In order to know the effect of DS concentration in flow rate, experiments have also been

179 carried out with different NaCl concentrations 250 mol/m^3, 500 mol/m^3, 750 mol/m^3,

180 1000 mol/m^3, 1500 mol/m^3, 2000 mol/m^3 and with different feed flows rate $5.0 \cdot 10^{-6}$

181 m^3/s, $6.7 \cdot 10^{-6}$ m^3/s, $8.3 \cdot 10^{-6}$ m^3/s, $10.0 \cdot 10^{-6}$ m^3/s, $11.7 \cdot 10^{-6}$ m^3/s maintaining constant

182 the difference of the flows of the feed and the draw solutions ($2.5 \cdot 10^{-6} m^3/s$). All

183 measurements were carried out at a temperature of 298 K.

184

185 *2.3 Emerging contaminants*

186 All target contaminants of emerging concern (CECs) were purchased from Sigma

187 Aldrich (Merck KGaA, Saint Louis, MO, USA), Fisher (Fisher Sci., Waltham, MA,

188 USA) and Scharlab (Scharlab, Barcelona, Spain). The list of contaminants is presented

189 in Table 2. All of them were prepared individually in stock solutions of 1000 mg/L in

190 methanol (MeOH), except for amoxicillin which was in MeOH/H_2O (1:1) and,

191 ciprofloxacin and ofloxacin which were in 0.2% HCl MeOH/H_2O (1:1). All of them

192 were saved in the freezer at -80 °C. Subsequently, each stock solution was diluted to 20

193 mg/L with MeOH and they were kept in the freezer at -20 °C until being used for the

194 experiments.

195 Molecular weights (MWs) as well as the octanol–water distribution coefficients (Kow)
196 were taken from SciFinder database. The octanol / water partition coefficient Kow, which
197 were used to determine the hydrophobic/hydrophilic character [41,42] of CECs,
198 represents the concentration ratio of a compound that partially dissolves between two
199 immiscible phases, one is octanol and the other is water. The octanol / water partition
200 coefficient is typically used as log Kow and it is positive when the species is hydrophobic,
201 since it means that more concentration is dissolved in octanol than in water.

202 The charge can be obtained from the acid / base equilibrium constants, since they allow
203 us to determine the dominant species at a given pH. In the case of charged species that
204 depend on the pH of the solution, the hydrophobic / hydrophilic character must consider
205 their presence. For this purpose, Tetko and Bruneau [43] defined the $\log D$ coefficient
206 that has been calculated for the compounds of this work (See table 2 and tables S-1 and
207 S-2 in the supplementary material):

208 $$\log D = \log K_{ow} - \log\left(1 + K_{+-}\right) \quad (3)$$

209 Where

210 $$\begin{aligned} K_{+-} &= 10^{(pH - pK_a)} \quad \text{for acids.} \\ K_{+-} &= 10^{(pK_a - pH)} \quad \text{for bases.} \\ K_{+-} &= 0 \quad \text{for neutrals.} \end{aligned} \quad (4)$$

211

212 **Table 2.** Properties of compounds**.**

Analytes	MW (amu)	log K_{ow} at 25 °C	log D	Charge pH 7
Ciprofloxacin	331.34	1.625	1.625	Neutral
Ofloxacin	361.37	1.855	1.855	Neutral
Sulfamethoxazole	253.28	0.659	-0.558	Negative
Metronidazole	171.15	-0.135	-0.135	Neutral
Erythromycin	733.93	1.909	0.720	Positive
Clarithromycin	747.95	2.805	1.616	Positive
Diclofenac	296.15	4.548	1.727	Negative
Naproxen	230.26	2.876	0.713	Negative

Ibuprofen	206.28	3.502	0.911	Negative
Salicylic acid	138.12	2.011	-1.979	Negative
Acetaminophen	151.16	0.475	0.475	Neutral
Clofibric acid	214.65	2.425	-1.395	Negative
Gemfibrozil	250.33	4.302	2.050	Negative
Carbamazepine	236.27	1.895	1.895	Neutral
Triclosan	289.54	5.343	5.343	Neutral
17-α- Ethinylestradiol (EE2)	296.40	4.106	4.106	Neutral
17-β-Estradiol (E2)	272.38	4.146	4.146	Neutral
Estrone (E1)	270.37	3.240	3.624	Neutral
Atenolol	266.34	0.335	-2.097	Positive
Iohexol	821.14	-2.921	-2.921	Neutral
Caffeine	194.19	-0.628	-0.628	Neutral
Crotamiton	203.28	2.464	2.464	Neutral
DEET	191.27	2.419	2.419	Neutral
Atrazine	215.68	2.636	2.636	Neutral

The experiments were carried out spiking milliQ (Merck KGaA, Saint Louis, MO, USA) water with each of analytes individually in FS and at 500 mol/m^3 NaCl in DS to find out the rejection of the membrane to each of the contaminants. Flow rates were set at $8.3 \cdot 10^{-6}$ m^3/s for FS and $5.8 \cdot 10^{-6}$ m^3/s for DS in all experiments. All measurements were performed at a pH around 7. Spiking levels were selected according to the average concentrations found for each analyte in the influent of sewage to European urban WWTPs, especially in Spain, published in the scientific literature [1, 2]. It is worth noting that the range of concentrations is of the same order at the entrance and exit of the WWTPs [1,2,13,14] because WWTPs are not designed to remove this type of pollutant. These concentrations ranged from 2 to 20 μg/L. System operation consisted of feeding 2 L of spiked DI water against 1 L of a 0.5 M NaCl solution in the draw until a reduction of the feeding volume of around 50% is achieved. This took around 14 minutes per batch although for times over 10 min the rejection of CECs remained already stationary. Samples were collected from FS at time 0 and, FS and DS at the end of the experiment, and immediately stored in the freezer at -20 °C until analysis. Afterwards, Afterwards, osmotic washes of the membrane were performed by placing

milliQ water in FS and DS for 14 minutes each wash. The washes were carried out to recover the part of the compound that has been retained inside the hollow fibers of the membrane. To know if the target analytes are retained on the membrane after the 14 minutes run, FS and DS samples were also collected after each wash for analysis. A total of 3 wash cycles were carried out, maintaining operational flow rates for both FS and DS.

2.4 Rejection rate calculations for CECs.

Rejections of CECs were calculated by equation (5) [36].

$$R = \left(1 - \frac{V_{DS\,end} C_{DS\,end}}{V_{total} \left(C_{FS\,0} + C_{FS\,end} \right) / 2} \right) \quad (5)$$

Where $V_{DS\,end}$ is the end volume of the draw, $C_{DS\,end}$ the end draw concentration, $C_{FS\,0}$ the initial feed concentration, $C_{FS\,end}$ the end feed concentration and V_{total} the total transported water volume. Here, this Equation will be applied, and R will be calculated, for an approximate 50% volume reduction in the feed solution.

2.5. Analytical Method

The samples were analyzed by Ultra-High-Performance Liquid Chromatography (UHPLC) – tandem Mass Spectrometry (MS/MS) in Selected Reaction Monitoring (SRM) mode. More specifically, the chromatographic separation was carried out by a Sciex Exion UHPLC (Danaher, Washington, DC, USA) and a Phenomenex (Danaher, Washington, DC, USA) reversed-phase column Kinetex EVO C18 (2.1 mm × 50 mm, particle size 1.7 μm), making use of H_2O and MeOH-based mobile phases containing 0.1% formic acid as modifier. The column was heated up to 40 °C. Injection flow rates

253 varied from 15 to 500 µL, depending on the analyte and its initial FS concentration, in
254 order to get optimum analytical conditions. Gradient flow rate was set at $8.3 \cdot 10^{-9}$ m^3/s
255 and total chromatographic run time was 10 min. Mass detection was performed by a Sciex
256 6500+ QqQ, both positive and negative electrospray ionization (ESI) modes in the same
257 run. The full list of SRM parameters is given in supplementary material (Table S-3).
258 Limits of detection (LOD) and quantification (LOQ) are shown in table S-4 of the
259 supplementary material.

260

261 **3. Results and discussion**

262 *3.1 FO membrane characterization with pure water feed*

263 The membrane module characterization along the experiments functioned practically
264 according to the manufacturer's specifications. The small deviations could be attributed
265 in part to batch-to-batch variability and other differences in the measurement
266 procedures. Moreover, it is not rare to find worst performances than these claimed by
267 the manufacturers. In any case, an average permeate flux value of $(2.33 \pm 0.19)\ 10^{-6}$ m/s
268 was obtained which is 23 % lower than that consigned by the manufacturer. Besides, a
269 reverse flow of salt of $(3.09 \pm 0.16)\ 10^{-6}$ mol/m^2s was obtained which is 61 % lower than
270 claimed by the manufacturer.

271 The manufacturer gives, for deionized water as feed and 0.5 M NaCl, with a feed rate of
272 25 L/h and a feed rate of 15 L/h as extraction rate, a specific salt flow of 0.15 ± 0.05
273 g/L. Here, under the same conditions, we got a specific salt flow Js/Jw = 0.08 g /L.
274 Values of the order of 0.11g /L are found in literature, see reference [37] (table 2) and
275 other authors[25,36], for similar modules of forward osmosis hollow fiber membranes
276 with aquaporins. Membranes with aquaporin favor water over NaCl flux giving

277 reasonably low specific salt fluxes. The values obtained here are fairly good when
278 compared to those reported for membranes without aquaporins [44, 45] who reported
279 Js/Jw, for NaCl solutions on the draw side, well over 0.15 g/L to about 0.5 g/L. Lower
280 specific salt flows would be obtained for other salts as $MgCl_2$, for example [45],
281 although these salts would be less convenient from an practical point of view.

282 The characterization of the membrane has been repeated after the experiments with all
283 the emerging contaminants studied here. It has been observed that the both the flow rate,
284 J_w, and reverse salt flow, J_s, remained practically constant what means that fouling is
285 very low.

286 *3.1.1 Effect of different feed and draw flow rates*

287 Experiments have been carried out with different feed and draw flow rates concentration
288 of NaCl was set at 500 mol/m^3. The corresponding Reynolds numbers show that in all
289 cases we have laminar regime on both sides of the membrane (See table S-5 in the
290 supplementary material where, as an example, the Reynolds number for FS are shown).
291 The aim is to determine the water flux provided by the membrane at different flow rates
292 inside the fibers. The maximum water flux for each of the feed flow rates used within
293 the membrane is obtained by extrapolating at time zero. Within the ranges tested flow
294 rates have a very limited effect on the water flux through the membrane. Note that, as
295 commented in section 2.2, in these experiments both the DS and FS are simultaneously
296 varied while keeping their difference constant.

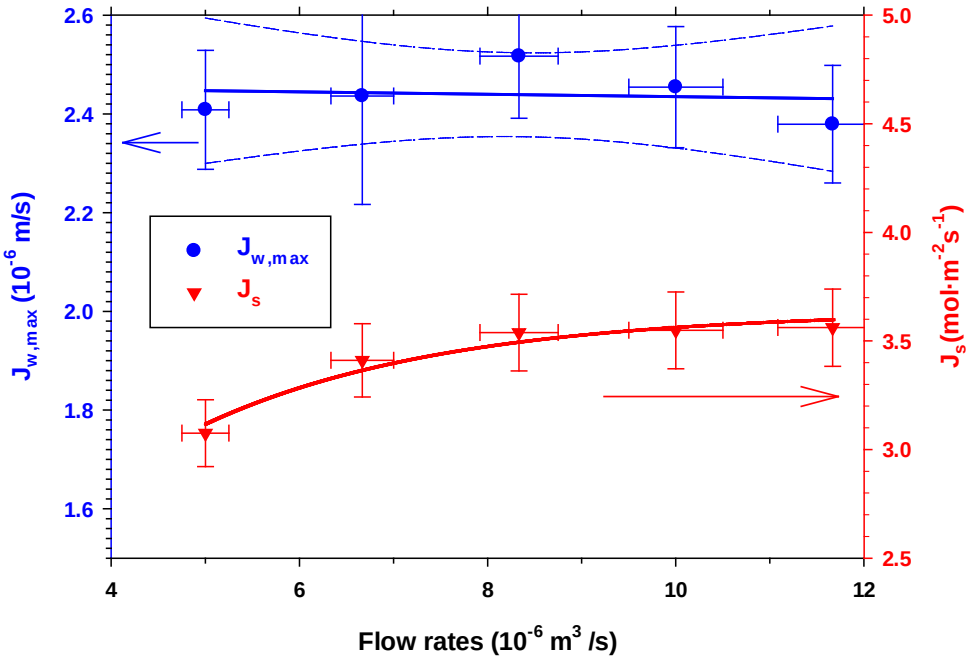

Figure 3. Maximum water flux, $J_{w,max}$ (left axis) and reverse salt flux, J_s (right axis) versus FS Flow rates.

297

298 As can be seen in Figure 2 (left axis), the permeate flux provided by the membrane is
299 practically constant, within the error range, in the range of tested feed flow rates. In
300 effect, it is observed that the linear regression fits the experimental data practically with
301 zero slope and all the points are within the 95% confidence interval. This can be due to
302 the constancy of osmotic pressure that controls the flow rate of permeate. In effect,
303 when osmotic pressure does not change, water flux must remain almost constant. This
304 would mean that the concentration polarization on the DS side would not be very
305 sensitive to velocity. This is reasonable, since this polarization occurs within the porous
306 matrix of the hollow fiber support and must not be affected significantly by the
307 tangential velocity to the surface of this.

308 The reverse salt flux at the end of the experiment has a slight upward trend as the flow
309 rate within the fibers increases as shown in Figure 2 (right axis). It is worth noting that

in this case a salt accumulation appears on the active layer of the membrane, which is efficiently swept by the tangential flow. As the salt flux in this type of system is mainly diffusive, less polarization means lower salt concentration in the FS side and higher saline flux, as long as the salt concentration within the porous layer of the membrane on the DS side can be considered constant [46].

Since J_w is not nearly sensitive to tangential flow, it can be thought that it is better to work at low speeds to reduce salt flow. However, since the objective is to use FO for the elimination of CECs, decreasing the tangential flow (at least on the FS side) would increase the polarization of the CECs, increasing the loss of CECs on the DS side. According to figure 2, from a flow of the order of 6.7 $.10^{-6}$ m^3/s, the saline flow remains almost constant, so something similar is expected to happen with the CECs.

3.1.2 Effect of NaCl concentration

Experiments were carried out maintaining the feed flow at $6.7 \cdot 10^{-6}$ m^3/s and the draw solution at $4.2 \cdot 10^{-6}$ m^3/s and changing the NaCl concentration from 250 mol/m^3 to 2000 mol/m^3. The objective of this experiment is to determine if there is an optimal NaCl ratio that allows a lower salt consumption. As in the previous experiment, the maximum permeate flow rate for each concentration of NaCl studied was obtained by extrapolating to zero time.

329 Figure 3 shows the trend of maximum water flux (left axis) and reverse salt flux (right

330 axis) as a function of DS bulk concentration. As expected, in both cases the behavior is

331 increasing with the concentration of DS, since an increase in osmotic pressure will

332 produce an increase in $J_{W,\max}$ and the increase in the concentration gradient between DS

333 and FS will increase the diffusive transport of salt, J_s

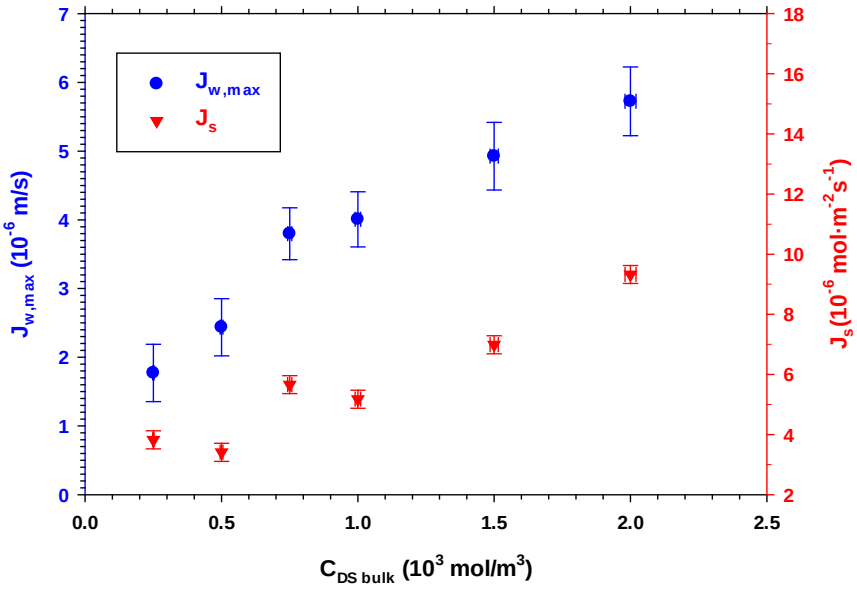

Figure 4. Maximum water flux (left axis) and reverse salt flux (right axis) versus concentration of salt in the bulk of the DS.

334 In FO, when the FS is in contact with the active layer and the DS with the support,

335 water flux can be calculated as [47]:

336 $$J_{w,\max} = L_p\left[\pi_{DS\,bulk}\exp\left(-J_{w,\max}K\right) - \pi_{FS\,m}\right] \quad (6)$$

337

338

Where L_p is the hydraulic permeability, $\pi_{DS\,bulk}$ is the osmotic pressure of the DS in the bulk and $\pi_{FS\,m}$ is the osmotic pressure of FS on the membrane surface, K is the solute resistivity for diffusion within the porous support layer, defined as [48]:

$$K = \frac{l\tau}{D\varepsilon} \tag{7}$$

Where l is the thickness of the active layer, τ the tortuosity ε porosity and D the diffusivity of the solute.

In our case $L_p = (3.78 \pm 0.07)10^{-12}\, m/sPa$ as determined by flow measurements against pressure in a range between 0.5 and 2.5 bar. Since in this case, $J_{w\,\max}$ corresponds to the extrapolation at zero time (not giving time to the passage of the solute next to the FS) we can assume that the salt concentration of FS in contact with the membrane should be zero and therefore, its osmotic pressure. In addition, given the low flows shown in Figure 2, the osmotic pressure of FS should be negligible compared to DS.

$$J_{w,\max} = L_p \pi_{DS\,bulk} \exp\left(-J_{w,\max} K\right) \tag{8}$$

The osmotic pressure can be determined from the Van't Hoff equation; since, for NaCl solutions below 2000 mol/m^3, the Van't Hoff estimates it with notable accuracy [46, 49]:

$$\pi_{DS\,bulk} = iR_g T C_{DS\,bulk} \tag{9}$$

Where i is the Van't Hoff factor, R_g is the universal constant of the gases, T the absolute temperature and $C_{DS\,bulk}$ the concentration of DS in the bulk.

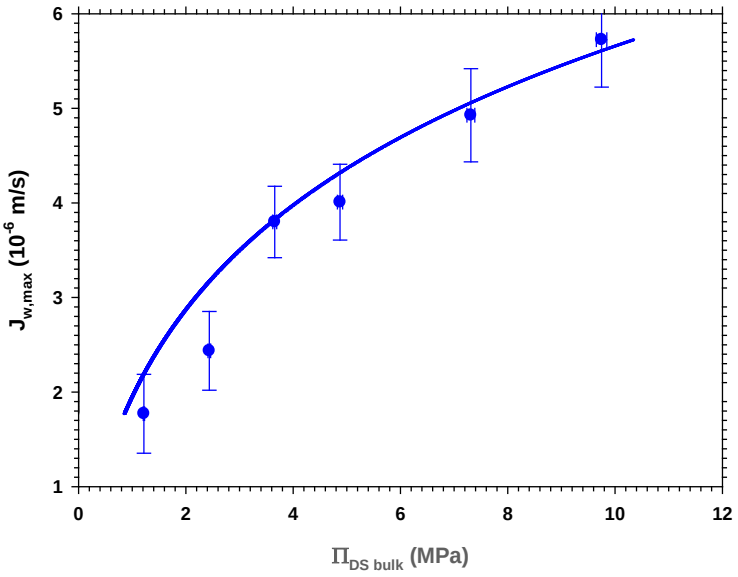

Figure 5. Maximum Water Flux Values versus DS Osmotic Pressure in Bulk. The curve corresponds to the fit of the data to the model (Equation (5)).

Figure 4 shows the values of $J_{w,\max}$ as a function of the osmotic pressure in the DS bulk. An adjustment to equation (8) allows us to determine the solute resistivity for diffusion within the porous support layer $K = (3.36 \pm 0.10)10^5 s/m$. It is appreciated that although there is a certain dispersion in the experimental data, the trend of the values is like that of the model. According to equation (7) if we multiply K by the diffusivity of the NaCl we obtain the value of a relation that only depends on geometric values of the membrane: $l\tau/\varepsilon = (4.99 \pm 1.4)10^{-4} m$. This value is very similar to the one found by other authors for FO membranes. [47].

368 It is observed that the model predicts an increase in $J_{w,\max}$ as the osmotic pressure (that
369 is, the concentration of DS) increases. However, the slope is decreasing, which makes
370 us weigh other factors such as saline flow and energy costs of increased tangential flow.
371 Figure 3 shows an approximately constant increase with concentration of DS in the
372 bulk. This is known as the diffusive Flow:

373 $$J_s = B\left[C_{DS\,m} - C_{FS\,m}\right] \tag{10}$$

374 Where *B* is the salt permeability coefficient of the active layer , $C_{DS\,m}$ and $C_{FS\,m}$ are
375 the salt concentration of the DS and FS in contact with the active layer of the membrane
376 respectively. According to McCutcheon and Elimelech [47]:

377 $$\begin{aligned} \pi_{DS\,m} &= \pi_{DS\,bulk} \exp\left(-J_{w,\max} K\right) \\ \pi_{FS\,m} &= \pi_{FS\,bulk} \exp\left(J_{w,\max} / k_m\right) \end{aligned} \tag{11}$$

378

where $\pi_{DS\,m}$ and $\pi_{FS\,m}$ are the osmotic pressures in contact with the active layer of the membrane on the DS and FS side respectively, and k_m is the mass transfer coefficient in the FS. Making use of Film Theory and using the Graetz-Leveque relationship [50] we

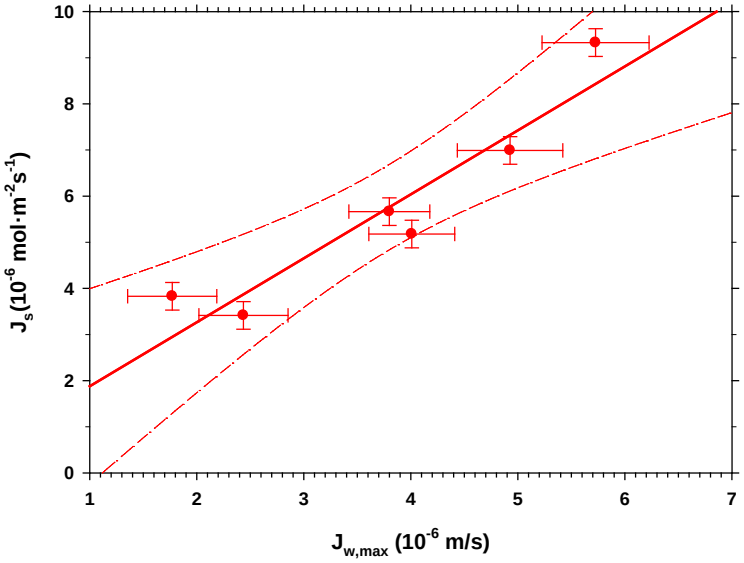

Figure 6. Reverse saline flux versus maximum water flux.

can determine k_m. Thus, the use of Van't Hoff's equation, the (11) equations, allows us to determine the concentrations of the solution on both sides of the active layer of the membrane. The adjustment of the saline flow against the difference of concentrations on both sides of the active layer of the membrane (equation (10)) allows us to determine the salt permeability coefficient of the active layer, $B = (2.83 \pm 1.3)10^{-8} m/s$ although with a wide range of uncertainty (see fig S-1) in supplementary material). However, taking into account equation (8) and considering despicable $C_{FS\,m}$ versus $C_{DS\,m}$ in the equation (10), the following relation is obtained [46]:

$$J_s = \frac{B}{AiR_gT} J_{w,\max} \quad (12)$$

This allows to determine the salt permeability coefficient of the active layer in a simpler way. Figure 5 shows this representation and the fit to the equation (12). In this case, $B = (2.6 \pm 0.5)10^{-8} m/s$. Value compatible with the one obtained by the previous method and with a lower level of accidental error. This value is in the lower range of the values found in the literature for FO [51]. The figure shows that the increase in water flux (produced by the increase in osmotic pressure) produces a linear increase in saline flow. This fact, together with the $J_{w,\max}$ curvature shown in Figure 4 and the increase in process costs incurred by increasing the salt concentration in the DS, suggests that a concentration of 500 mol/m^3 of NaCl may be appropriate for the process of concentrating CECs by FO.

3.2 Rejection of CECs

These experiments have been performed with a feed flow of $8.3 \cdot 10^{-6}$ m^3/s and draw solution flow of $5.8 \cdot 10^{-6}$ m^3/s with a NaCl concentration of 500 mol/m^3. A concentration of 500 mol/m^3 has been chosen because it is similar to that of sea water. The circulation flows on the FS and DS were chosen, in accordance with Figure 2, when J_S and J_W are almost constant and CECs concentration polarization is fairly small by simultaneously keeping energy costs down. Rejection of each emerging contaminant was evaluated by using Equation (5), when 50% of the feed volume reduction had been achieved. The experiments were performed for each compound separately in the feed solution, with a concentration in the interval between 2-20 μg/L depending on each compound and always considering similar concentrations to those found in the literature for these compounds. The spiking concentration of each compound is shown in table S-2 of the supplementary material. Figure 6 shows the percentage of rejection for the 24

414 contaminants tested, divided into three groups according to their charge at pH=7 (See
415 table 2). All the compounds were found to be at least 93% rejected and 19 of them have
416 rejections greater than 99%. This was expected as the rejection of this type of
417 substances in this kind of membranes, with a certain porous structure and chemical
418 nature, is related to their MW, electrical charge and hydrophilic/hydrophobic character
419 of the permeating solutes [52].

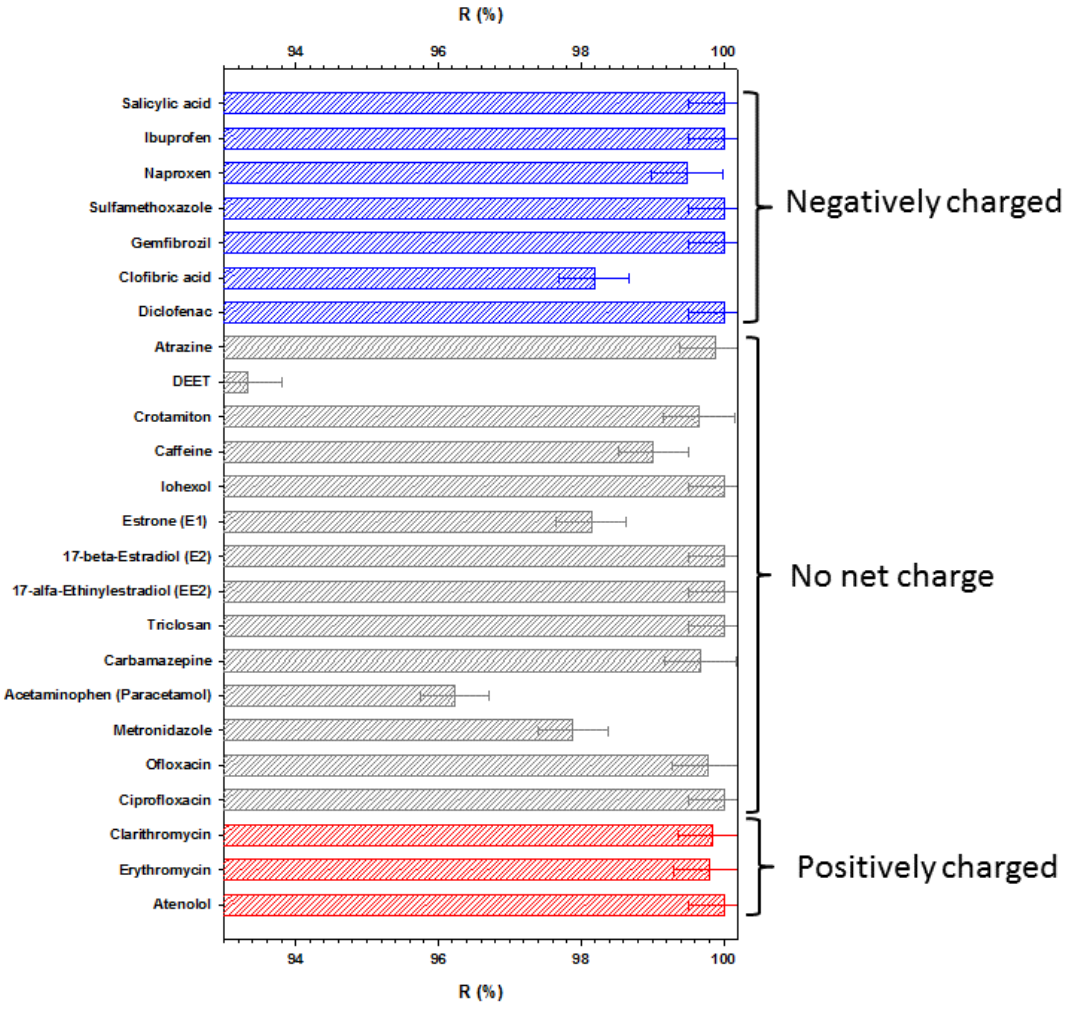

420

421 **Figure 6.** Rejection of contaminants grouped according to their charge at pH=7.

422 Figure 7 shows the influence of these parameters on the rejection of all the analytes
423 sorted out by their polarity at pH 7 (positive, negative, and neutral). A clear dependence
424 on the molecular weight was observed. It can also be appreciated, for neutral or

425 negatively charged molecules, a tendency to increase rejection with the hydrophobic
426 character of the substance. Compounds with lower rejection such as DEET,
427 Metronidazole and Acetaminophen as can be seen in figure 6 have in common the low
428 molecular weight and the lack of any net charge. Small molecules might be able to
429 reach the porous structure in the membrane active layer and get a larger adsorption
430 surface. Since they have a lower molecular weight, they are easier to pass through the
431 membrane. However, in the case of Atenolol (MW=266.34) that has a positive charge,
432 we obtained a higher rejection than expected based on its MW. This should be due to
433 the deposition of part of the compound on the active layer [53] which is negatively
434 charged. In fact, a membrane from the same manufacturer with a larger area but with
435 the same type of hollow has an isoelectric point is at 3.7 [37, 39]. An isoelectric point in
436 the range from 2 to 4 was expected due to the carboxylic groups at the surface of the
437 polyamide [54]. This would be reflected in a decrease in concentration in the permeate,
438 more pronounced in systems with small feed concentrations, as in this case. Equation
439 (5) would give lower rejections than those expected as in this case, and they would
440 increase when the system completely reached the stationary status as other authors have
441 observed. [52, 53]. With an analysis of the global loss of mass in the system, as we will
442 do in the following section, this behavior can be corroborated. Either way, it seems
443 reasonable to admit that the imperfect fitting of rejection on MW and log D can be
444 attributed to possible specific chemical or physical interactions of the contaminants with
445 the membrane.
446

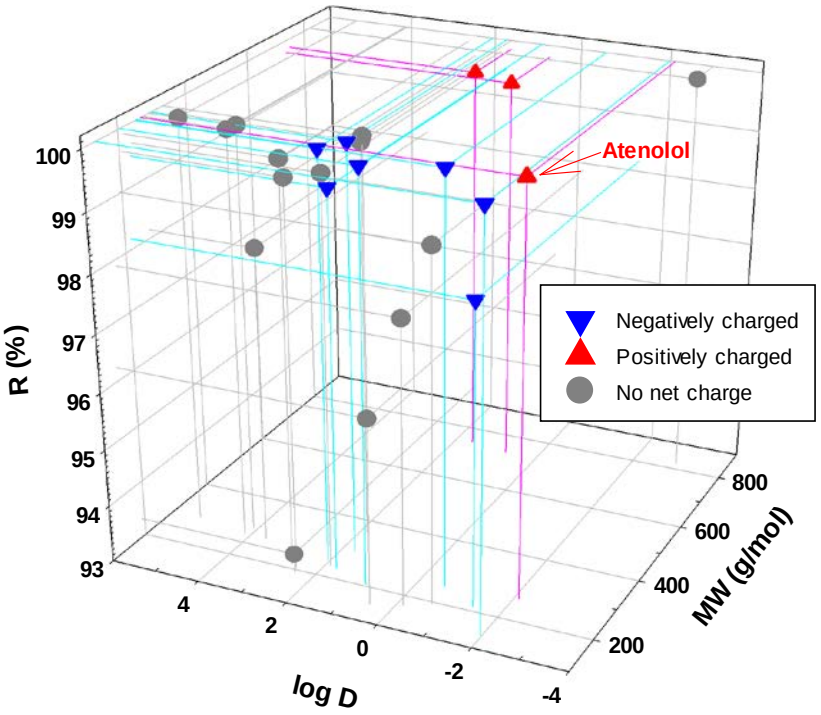

Figure 7: Rejection according to the molecular weight and the hydrophobic/hydrophilic character of the permeating substances.

There are several studies with forward osmosis membranes that examine the rejection of emerging contaminants. Some studies have been performed using cellulose triacetate (CTA) membranes. Kim et al. (2018) found that for the charged compounds (Atenolol, Ibuprofen, Naproxen, Gemfibrozil, Sulfamethoxazole and Diclofenac), rejections between 80-98% were obtained. For nonionic compounds (such as Carbamazepine, Estrone, 17 α-Ethynilestradiol, Paracetamol, Metronidazole, Clofibric acid, DEET and Caffeine) Kim et al. obtained rejections between 40-98% [55]. Gao et al. (2018) studied

458 the rejections of four contaminants with a CTA membrane and found rejections for two
459 of our studied hormones (E1 and E2) between 77-99.9% [56].

460 However, previous studies have shown that TFC FO membranes, in addition to
461 achieving higher water flux, also achieve better contaminant rejection than cellulose
462 triacetate (CTA) FO membranes [31,55,57,58].

463 There are more limited studies of the rejection of contaminants by a TFC membrane.
464 All of them use a hollow fiber configuration for the FO TFC membrane. Nikbakht et al.
465 (2020) found a high rejection in contaminants such as 2–6 dichloro-benzamide (BAM),
466 2-methyl-4-chlorophenoxyacetic acid (MCPA) and 2- (4-chloro-2-methylphenoxy)
467 propionic acid (MCPP) (> 97%) [37]. Engelhardt et al. (2018) had a high rejection in
468 2,4-dichlorophenoxyacetic acid (2,4-D), bisphenol A (BPA) and methyl paraben (>
469 95%) [36].

470 Therefore, if we comparing the previous rejections obtained with a FO flat CTA
471 membrane with our results with the FO Aquaporin HF membrane, it is observed that we
472 obtained better rejections for the same contaminants studied. Nonetheless, results with
473 hollow fiber forward osmosis TFC membranes cannot be compared because they are
474 much scarcer up to now.

475 The results of saline flux and water flux do not present significant variations with the
476 type of contaminant and neither is there a trend that can be related to the molecular
477 weight, the electrical charge or the hydrophobic/hydrophilic character (see fig S-2 and
478 S-3) in supplementary material). The mean value with its standard deviation for all
479 experiences with CECs is (2.28 ± 0.28) 10^{-6}mol/m^{2}s for NaCl flow (J_s) and (2.05 ±
480 0.12). 10^{-6} m/s for J_w. There is a decrease in the average values of 36% for J_s and 16%

for J_w, compared to the values obtained with pure water in FS, at the same salt concentration in DS and the same speeds (See fig 2).

It seems clear that the presence of the CECs produces a decrease in both flows. On the one hand, the saline and water diffusion should decrease due to the presence of the other solute. In addition, the possible adsorption of the CECs could reduce the effective size of the pores (and even cause their blockage), producing a reduction of both flows. In the following section, we will see that adsorption is an important phenomenon, which is present in these experiences.

We should not forget that the rejection values of the CECs shown are calculated as an average value. In addition, we must consider that it is an observed rejection, since there will be polarization of the concentration near the surface of the membrane. This polarization will depend on the concentration of CEC in the FS and the water flux, J_w, (i.e., the concentration of NaCl in the DS), for certain conditions of tangential flow in the DS and FS. To see if this effect is important in our system, rejection measurements were made at two concentrations of CECs in FS (3 and 10 ppm) and two concentrations of NaCl in DS (500 mol/m^3 and 1000 mol/m^3) for three of the previous CECs: Clofibric acid, Atenolol and Diclofenac) maintaining the conditions of the tangential flow equal to those used for the rest of the CECs in this section.

No significant differences (or trends) were observed with the change of any of the variables. The values of the standard deviations between the different conditions measured are less than the experimental error inherent in the measurement (see table S-

502 2 and fig S-4 in the supplementary material). This is to be expected, since the decrease
503 in the feed concentration considerably reduces its polarization [59].

504 Finally, it is worth mentioning that, although an adsorption of some CEC within the
505 matrix of the membrane could modulate initial rejection, we have not detected it. This
506 could be due to a very fast kinetics of such initial adsorption step. Anyway, the
507 corresponding fluctuation would be within the error range.

508 *3.3 Recovery of CECs in the different stages*

509 It was observed, in the previous section that although all the compounds tested showed
510 rejections very close to 100 %, and even when rejection is 100 %, the compound was
511 not completely recovered in the feed solution. This phenomenon has already been
512 observed by other authors for some of the compounds used in this work in a
513 nanofiltration aromatic polyamide membrane [53]. This may imply that a significant
514 part of the compounds tested may be retained inside the membrane fibers. In order to
515 determine whether internal retention occurs, three washings of the membrane with
516 MilliQ water was performed for each contaminant under the same conditions and with
517 the same flow rate in order to recover the CECs internally retained. Samples were taken
518 from the feed solution and from the draw solution. As can be seen in Figure 8, in the
519 initial experiment (Test FS+ Test DS) the percentage of recovery of each compound
520 varies between 50% and 70% except for Ciprofloxacin, Triclosan and Atenolol which
521 only were recovered around 35%. As it is shown in the figure, most of the contaminants
522 were recovered after the first wash, in the second wash the recovery percentage was
523 very low, and the third wash would not be necessary. The data obtained for rejection in
524 the previous section show that the aquaporin hollow fiber membrane can reject more
525 than 93 % of the 24 emerging contaminants analyzed. However, there may be important
526 interactions between the material of the fibers and the tested compounds, which makes

the retention inside the membrane an important factor to be considered, being necessary to carry out two washes to completely recover each contaminant.

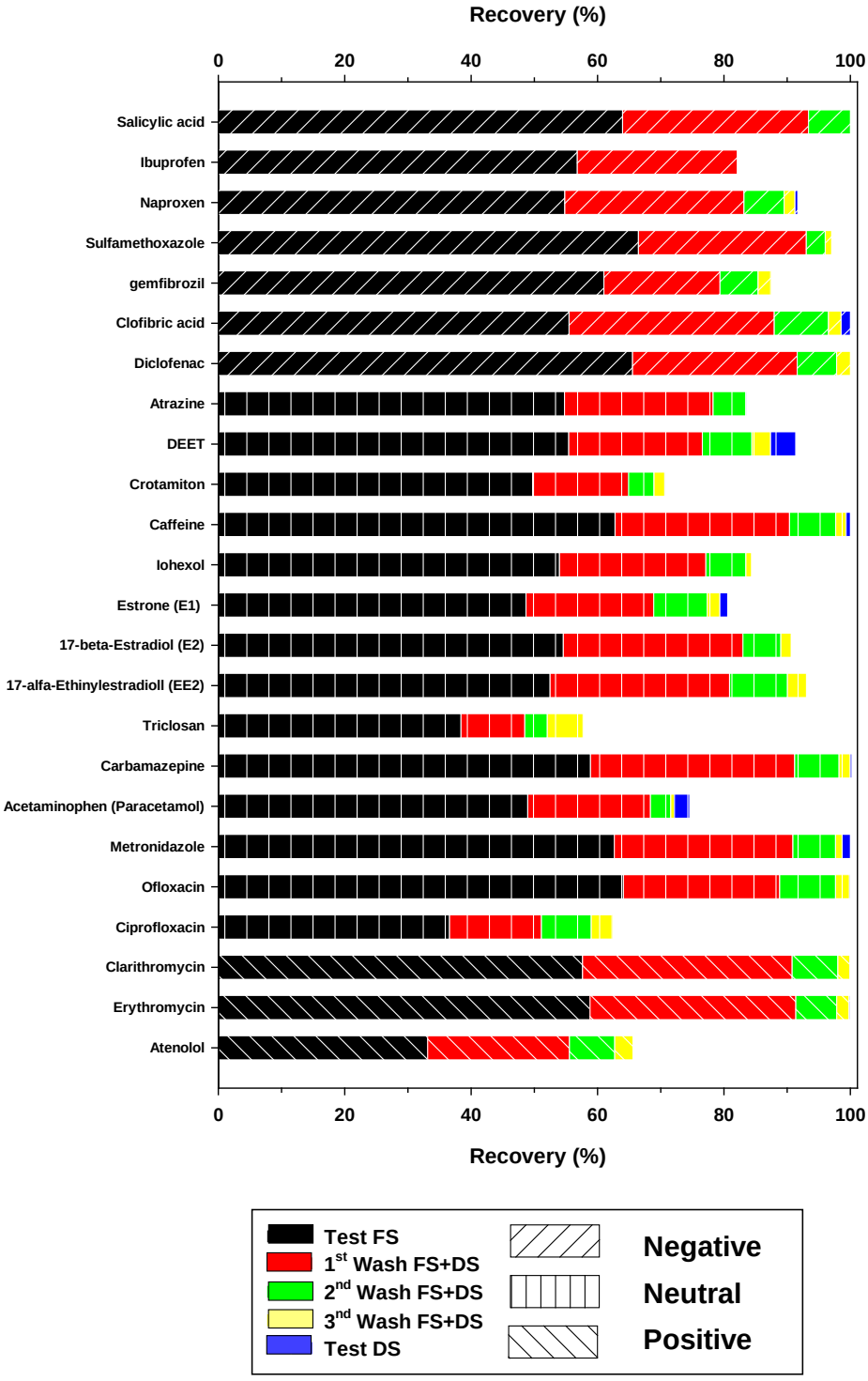

Figure 8. Recovery in the different stages.

To analyze the influence of solute adsorption on the porous matrix (as in the case of retention analysis) we have analyzed its behavior as a function of the molecular weight and the log D coefficient. Figure 9 shows the mass of solute recovered in the FS after the rejection test. We consider that this recovery is the most correlated with the adsorption active sites, while the recovery after the washing must be more related to the strength of the interaction between the solute and the membrane. There is a very clear trend between adsorption (low recovery) and low molecular weight. Compounds of lower molecular weight can enter into the porous structure of the active layer and therefore have a larger adsorption surface. However, this adsorption also depends on the interaction between the compound and the membrane. A clear case is atenolol, which at pH=7 must have positive character. As it has a low molecular weight it must be able to penetrate more easily than other compounds in the porous matrix. Nevertheless, their rejection is 100% and their recovery is the lowest. This fits with the negative charge of the membrane that interacts with the positive molecules of the compound giving a recovery of less than 34%. Although later, with the washings recovering increases substantially, this recovery tends to be proportional to that of the first one. So that the three CECs that are most adsorbed in the rejection test are the farthest away from full recovery after the three washes. This should imply a strong solute-membrane interaction. Although as we see in this case there is no relation with log D for these three compounds (see table 2).

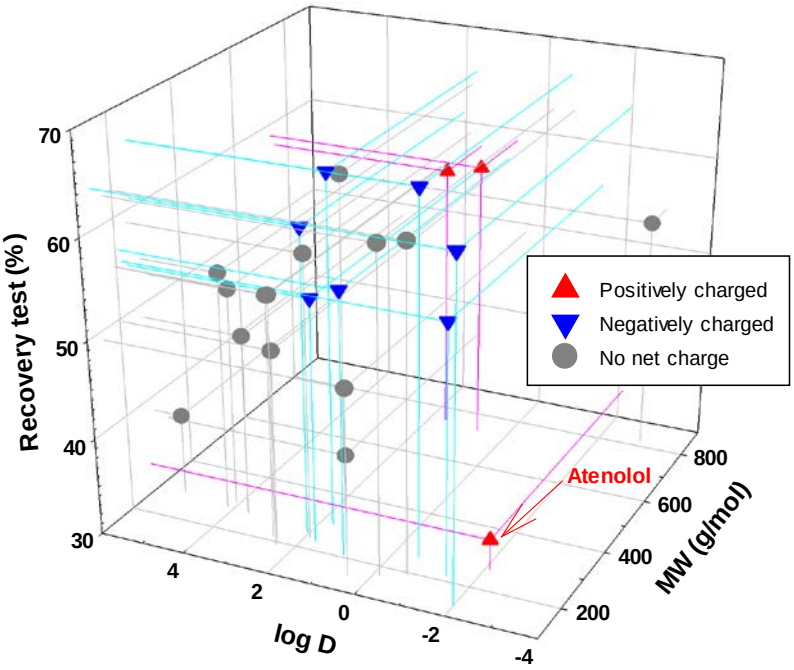

Figure 9: Recovery in the FS of the different CECs after the rejection test against the molecular weight and log D.

552

553 An analysis of the recovery capacity of the CECs was also performed as a function of
554 the CEC concentration in the FS and the NaCl concentration in the DS. The same three
555 CECs were studied as in the case of retention: Clofibric acid, Diclofenac and Atenolol.
556 In the case of the two compounds with a negative charge at pH = 7 (Clofibric acid and
557 Diclofenac, see table 2) no significant trends were observed and the differences were
558 attributed to experimental deviations. The total recovery of both is close to 100% for all
559 the conditions analyzed (similar to what is seen in Figure 8). In the case of Atenolol, a
560 compound that as we have mentioned has a positive charge at pH=7, it does present a
561 significant increase in recovery when the concentration of the compound in FS is
562 increased, as shown in figure 10. In these figures recovery for several experiments with
563 different feed solution (atenolol) and draw solution (NaCl) concentrations and
564 consecutive washings.

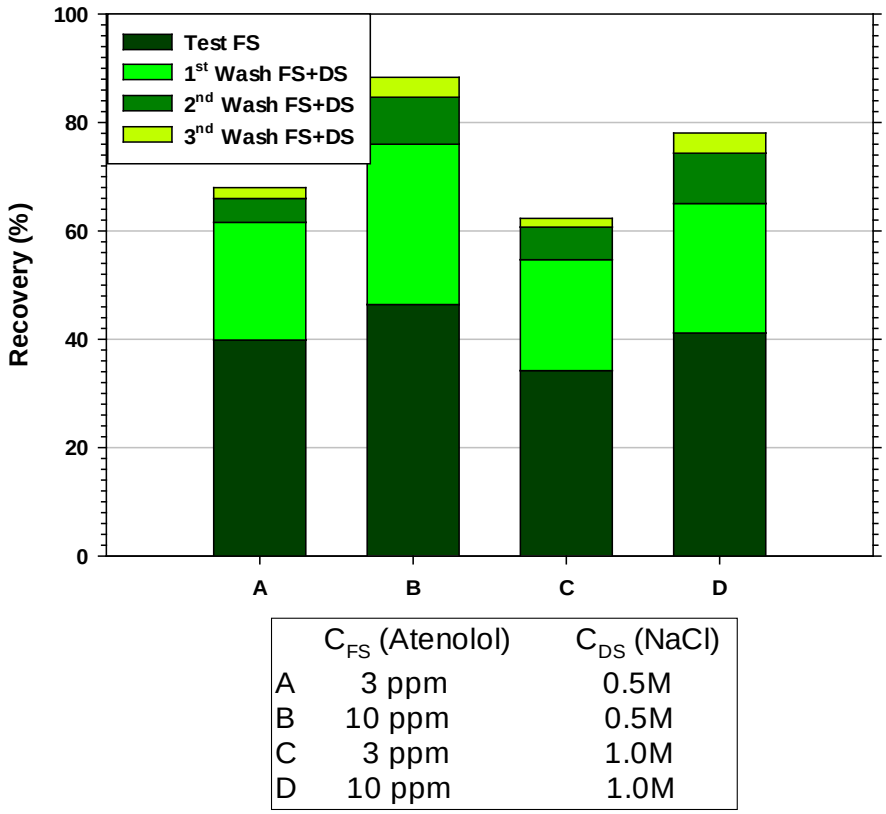

Figure 10: Recovery of Atenolol after the rejection test and after several washings. Experiments have been made with different concentrations of atenolol in FS and with different concentrations of NaCl in DS.

We have already commented that the low recovery of this compound must be related to its positive charge and its small size. Under these conditions, the compound can access the negatively charged sites of the membrane matrix, producing a stable bond. When the concentration of the compound in FS increases, most of the negative sites have already been occupied and Atenolol ceases to be accumulated within the porous matrix of the membrane. A decrease in recovery is also observed when the concentration of NaCl in the DS is increased. This increase in concentration we have seen produces an increase in J_w and J_s (see fig 3). The increase in J_w will facilitate the flow of Atenolol into the porous matrix and the increase in J_s will increase the concentration of NaCl within the

porous matrix by modifying the electrical double layer and the surface charge distribution. This double effect must be responsible for the greater affinity of Atenolol for the surface of the membrane when the concentration of DS is increased.

Previous studies confirmed that diffusion was the mechanism responsible for the rejection of aquaporin membrane contaminants through the FO system [23,26]. In fact, the increase in the rejection of the contaminant became less pronounced with the increase in the concentration of the draw solution (from 0.5 M to 1.0 M NaCl), according to these studies. This seems consistent with the solution-diffusion mechanism. In our case, due to the high retention values of the compounds studied we have not been able to analyze this behavior. However, the decrease of the Atenolol recovery (higher penetration in the porous matrix) with the increase of the driving force seems to confirm this behavior.

4. Conclusions

The research carried out shows that a high rejection of the different pollutants studied can be achieved when using a hollow fiber forward osmosis aquaporin module. It was possible to report a rejection higher than 99% for Ciprofloxacin, Ofloxacin, Sulfamethoxazole, Erythromycin, Clarithromycin, Diclofenac, Naproxen, Ibuprofen, Salicylic acid, Gemfibrozil, Carbamazepine, Triclosan, 17-α -Ethinylestradiol (EE2), 17-β-Estradiol (E2), Atenolol, Iohexol, Caffeine, Crotamiton and Atrazine. For Metronidazole, Acetaminophen, Clofibric acid, Estrone (E1) and DEET, minor rejects were obtained but over 93% in any case. Membrane rejection was probably influenced by the molecular dimensions, loading and membrane adsorption behavior of the organic contaminants tested. It is expected that, for a membrane with a certain porous structure

and chemical nature, the retention of this type of substances is related to its molecular weight (MW), its electrical charge and its hydrophilic/hydrophobic character of the permeating solutes. We could say that the aquaporin hollow fiber membrane is excellent in rejecting contaminants, but global mass balance indicates that a part of CECs is trapped due to adsorption within the porous matrix of the membrane. Hence, up to two full rinses were necessary to fully recover each contaminant. There is a very clear relationship between adsorption (low recovery) and low molecular weight. Small molecules might be able to reach the porous structure in the membrane active layer and get a larger adsorption surface.

5. Acknowledgements

This work was supported by the Regional Government of Castilla y León and the EU-FEDER (INFRARED-2018-UVA3, CLU 2017-09, VA088G19 and UIC 071 and UIC 082). Authors would like to thank the “Ministerio de Ciencia e Innovación” for the financial support through the research project PID2019-109403RB-C21. Furthermore, we would like to thank Aquaporin A/S (Copenhagen, Denmark) for providing detailed information about the product HFF06 and, Silvia Gallego as a technician in the laboratory of the Applied Physics department from the Porous Materials and Surfaces group (SMAP) at University of Valladolid where the experimental set-up was located. The analysis of CECs was carried out in the Laboratory of Instrumental Techniques (LTI) from the University of Valladolid (UVa).

6. References

[1] N.H. Tran, K.Y.H. Gin, Occurrence and removal of pharmaceuticals, hormones, personal care products, and endocrine disrupters in a full-scale water reclamation plant, Science of the Total Environment. 599–600 (2017) 1503–1516. https://doi.org/10.1016/j.scitotenv.2017.05.097.

[2] Y. Luo, W. Guo, H. Ngo, L.D. Nghiem, I. Hai, J. Zhang, S. Liang, X.C. Wang, A review on the occurrence of micropollutants in the aquatic environment and their fate and removal during wastewater treatment, Sci Total Environ, 473–474 (2014) 619–641, http://dx.doi.org/10.1016/j.scitotenv.2013.12.065.

[3] M.O. Barbosa, A.R. Ribeiro, M.F.R. Pereira, A.M.T. Silva, Eco-friendly LC–MS/MS method for analysis of multi-class micropollutants in tap, fountain, and well water from northern Portugal, Analytical and Bioanalytical Chemistry. 408 (2016) 8355–8367. https://doi.org/10.1007/s00216-016-9952-7.

[4] COMMISSION IMPLEMENTING DECISION (EU) 2015/495 of 20 March 2015 establishing a watch list of substances for Union-wide monitoring in the field of water policy pursuant to Directive 2008/105/EC of the European Parliament and of the Council. Off. J. Eur. Union L78, 40-42.

[5] DIRECTIVE 2013/39/EU OF THE EUROPEAN PARLIAMENT AND OF THE COUNCIL of 12 August 2013 amending Directives 2000/60/EC and 2008/105/EC as regards priority substances in the field of water policy. Off. J. Eur. Union L226, 1-17.

[6] DIRECTIVE 2000/60/EC, 2000. DIRECTIVE 2000/60/EC OF THE EUROPEAN PARLIAMENT AND OF THE COUNCIL of 23 October 2000 establishing a framework for Community action in the field of water policy. Off. J. Eur. Communities 327, 1-72.

[7] M. Carere, S. Polesello, R. Kase, B.M. Gawlik, The Emerging Contaminants in the Context of the EU Water Framework Directive. Emerging Contaminants in River Ecosystems. The Handbook of Environmental Chemistry, (2015) 197-215, https://doi.org/10.1007/698_2015_5011

[8] Ankley, G.T.; Hoff, D.J.; Mount, D.R.; Lazorchak, J.; Beaman, J.; Linton, T.K.; Erickson, R.J. Aquatic Life Criteria for Contaminants of Emerging Concern; OW/ORD Emerging Contaminants Workgroup; EPA: Boston, MA, USA, 2008, 1–46.

[9] A. Stefanakis, J. Becker, A Review of Emerging Contaminants in Water: Classification, Sources, and Potential Risks, 3 (2015) 57-82, https://doi.org/10.4018/978-1-4666-9559-7.ch003

[10] P. Burkhardt-Holm, Linking Water Quality to Human Health and Environment: The Fate of Micropollutants Working Paper Series, 2011. www.lkyspp.nus.edu.sg/iwp.

[11] D. Fatta-Kassinos, C. Manaia, T.U. Berendonk, E. Cytryn, J. Bayona, B. Chefetz, J. Slobodnik, N. Kreuzinger, L. Rizzo, S. Malato, L. Lundy, A. Ledin, COST Action ES1403: New and Emerging challenges and opportunities in wastewater REUSe (NEREUS), Environmental Science and Pollution Research. 22 (2015) 7183–7186. https://doi.org/10.1007/s11356-015-4278-0.

[12] I. Michael, L. Rizzo, C.S. McArdell, C.M. Manaia, C. Merlin, T. Schwartz, C. Dagot, D. Fatta-Kassinos, Urban wastewater treatment plants as hotspots for the release of antibiotics in the environment: A review, Water Research. 47 (2013) 957–995. https://doi.org/10.1016/j.watres.2012.11.027.

[13] J.O. Tijani, O.O. Fatoba, O.O. Babajide, L.F. Petrik, Pharmaceuticals, endocrine disruptors, personal care products, nanomaterials and perfluorinated pollutants: a review, Environmental Chemistry Letters. 14 (2016) 27–49. https://doi.org/10.1007/s10311-015-0537-z.

[14] J. Wilkinson, P.S. Hooda, J. Barker, S. Barton, J. Swinden, Occurrence, fate and transformation of emerging contaminants in water: An overarching review of the field, Environmental Pollution. 231 (2017) 954–970. https://doi.org/10.1016/j.envpol.2017.08.032.

[15] A.M. Gorito, A.R. Ribeiro, C.M.R. Almeida, A.M.T. Silva, A review on the application of constructed wetlands for the removal of priority substances and contaminants of emerging concern listed in recently launched EU legislation, Environmental Pollution. 227 (2017) 428–443. https://doi.org/10.1016/j.envpol.2017.04.060.

[16] P. Westerhoff, Y. Yoon, S. Snyder, E. Wert, Fate of endocrine-disruptor, pharmaceutical, and personal care product chemicals during simulated drinking water treatment processes, Environmental Science and Technology. 39 (2005) 6649–6663. https://doi.org/10.1021/es0484799.

[17] Y. Yoon, P. Westerhoff, S.A. Snyder, E.C. Wert, Nanofiltration and ultrafiltration of endocrine disrupting compounds, pharmaceuticals and personal care products, Journal of Membrane Science. 270 (2006) 88–100. https://doi.org/10.1016/j.memsci.2005.06.045.

[18] Y.A.J. Al-Hamadani, K.H. Chu, J.R.V. Flora, D.H. Kim, M. Jang, J. Sohn, W. Joo, Y. Yoon, Sonocatalytical degradation enhancement for ibuprofen and sulfamethoxazole in the presence of glass beads and single-walled carbon nanotubes, Ultrasonics Sonochemistry. 32 (2016) 440–448. https://doi.org/10.1016/j.ultsonch.2016.03.030.

[19] C. Jung, J. Park, K.H. Lim, S. Park, J. Heo, N. Her, J. Oh, S. Yun, Y. Yoon, Adsorption of selected endocrine disrupting compounds and pharmaceuticals on activated biochars, Journal of Hazardous Materials. 263 (2013) 702–710. https://doi.org/10.1016/j.jhazmat.2013.10.033.

[20] J. Han, Y. Liu, N. Singhal, L. Wang, W. Gao, Comparative photocatalytic degradation of estrone in water by ZnO and TiO2 under artificial UVA and solar irradiation, Chemical Engineering Journal. 213 (2012) 150–162. https://doi.org/10.1016/j.cej.2012.09.066.

[21] S.S. Sablani, M.F.A. Goosen, R. Al-Belushi, M. Wilf, Concentration polarization in ultrafiltration and reverse osmosis: a critical review, Desalination.141 (2001) 269–289.

[22] Blandin. G, Ferrari. F, Lesage. G, Le-Clech. P, Héran. M, Martinez-Lladó. X, Forward osmosis as concentration process: Review of opportunities and challenges, Membranes, (2020), 1-40, 10(10). https://doi.org/10.3390/membranes10100284.

[23] H.T. Madsen, N. Bajraktari, C. Hélix-Nielsen, B. van der Bruggen, E.G. Søgaard, Use of biomimetic forward osmosis membrane for trace organics removal, Journal of Membrane Science. 476 (2015) 469–474. https://doi.org/10.1016/j.memsci.2014.11.055.

[24] T.Y. Cath, A.E. Childress, M. Elimelech, Forward osmosis: Principles, applications, and recent developments, Journal of Membrane Science. 281 (2006) 70–87. https://doi.org/10.1016/j.memsci.2006.05.048.

[25] S. Engelhardt, J. Vogel, S.E. Duirk, F.B. Moore, H.A. Barton, Urea and ammonium rejection by an aquaporin-based hollow fiber membrane, Journal of Water Process Engineering. 32 (2019). https://doi.org/10.1016/j.jwpe.2019.100903.

[26] M. Xie, W. Luo, H. Guo, L.D. Nghiem, C.Y. Tang, S.R. Gray, Trace organic contaminant rejection by aquaporin forward osmosis membrane: Transport mechanisms and membrane stability, Water Research. 132 (2018) 90–98. https://doi.org/10.1016/j.watres.2017.12.072.

[27] B.D. Coday, B.G.M. Yaffe, P. Xu, T.Y. Cath, Rejection of trace organic compounds by forward osmosis membranes: A literature review, Environmental Science and Technology. 48 (2014) 3612–3624. https://doi.org/10.1021/es4038676.

[28] M. Xie, L.D. Nghiem, W.E. Price, M. Elimelech, Comparison of the removal of hydrophobic trace organic contaminants by forward osmosis and reverse osmosis, Water Research. 46 (2012) 2683–2692. https://doi.org/10.1016/j.watres.2012.02.023.

[29] A.A. Alturki, J.A. McDonald, S.J. Khan, W.E. Price, L.D. Nghiem, M. Elimelech, Removal of trace organic contaminants by the forward osmosis process, Separation and Purification Technology. 103 (2013) 258–266. https://doi.org/10.1016/j.seppur.2012.10.036.

[30] N.T. Hancock, P. Xu, D.M. Heil, C. Bellona, T.Y. Cath, Comprehensive bench- and pilot-scale investigation of trace organic compounds rejection by forward osmosis, Environmental Science and Technology. 45 (2011) 8483–8490. https://doi.org/10.1021/es201654k.

[31] J.C. Ortega-Bravo, G. Ruiz-Filippi, A. Donoso-Bravo, I.E. Reyes-Caniupán, D. Jeison, Forward osmosis: Evaluation thin-film-composite membrane for municipal sewage concentration, Chemical Engineering Journal. 306 (2016) 531–537. https://doi.org/10.1016/j.cej.2016.07.085.

[32] S. Sahebia, M. Sheikhic, B. Ramavandid, A new biomimetic aquaporin thin film composite membrane for forward osmosis: Characterization and performance assessment, Desalination and Water Treatment, 148 (2019) 42–50, https://doi.org/10.5004/dwt.2019.23748

[33] C.Y. Tang, Y. Zhao, R. Wang, C. Hélix-Nielsen, A.G. Fane, Desalination by biomimetic aquaporin membranes: Review of status and prospects, Desalination. 308 (2013) 34–40. https://doi.org/10.1016/j.desal.2012.07.007

[34] Li. Z, Valladares Linares. R, Bucs. S, Fortunato. L, Hélix-Nielsen. C, Vrouwenvelder. J, Ghaffour. N, Leiknes. T, Amy. G, Aquaporin based biomimetic membrane in forward osmosis: Chemical cleaning resistance and practical operation, Desalination, (2017), 208-215, 420, https://doi.org/10.1016/j.desal.2017.07.015.

[35] Kumar. M, Grzelakowski. M, Zilles. J, Clark. M, Meier. W, Highly permeable polymeric membranes based on the incorporation of the functional water channel protein Aquaporin Z, Proc. Natl. Acad. Sci. U. S. A., 104 (2007), 20719-20724, www.pnas.orgcgidoi10.1073pnas.0708762104.

[36] S. Engelhardt, A. Sadek, S. Duirk, Rejection of trace organic water contaminants by an Aquaporin-based biomimetic hollow fiber membrane, Separation and Purification Technology. 197 (2018) 170–177. https://doi.org/10.1016/j.seppur.2017.12.061.

[37] M. Nikbakht Fini, H.T. Madsen, J.L. Sørensen, J. Muff, Moving from lab to pilot scale in forward osmosis for pesticides rejection using aquaporin membranes, Separation and Purification Technology. 240 (2020). https://doi.org/10.1016/j.seppur.2020.116616.

[38] Zhao. Y, Qiu. C, Li. X, Vararattanavech. A, Shen. W, Torres. J, Hélix-Nielsen. C, Wang. R, Hu. X, Fane. A, Tang. C, Synthesis of robust and high-performance aquaporin-based biomimetic membranes by interfacial polymerization-membrane preparation and RO performance characterization, Journal of Membrane Science, (2012), 422-428, 423-424, https://doi.org/10.1016/j.memsci.2012.08.039.

[39] Sanahuja-Embuena. V, Khensir. G, Yusuf. M, Andersen. M, Nguyen. X, Trzaskus. K, Pinelo. M, Helix-Nielsen. C, Role of operating conditions in a pilot scale investigation of hollow fiber forward osmosis membrane modules, Membranes, (2019), 9(6), https://doi.org/10.3390/membranes9060066.

[40] J. Ren, JR. McCutcheon, Making thin film composite hollow fiber forward osmosis membranes at the module scale using commercial ultrafiltration membranes, Industrial & Engineering Chemistry Research 56 (14) (2017), 4074-4082, https://doi.org/10.1021/acs.iecr.6b04931

[41] C. Hansch, D. Rockwell, Y.C. Jow, A. Leo, E. Steller, Substituent constants for correlation analysis, Journal of Medicinal Chemistry 20-2 (1977).

[42] M. Ringpfeil, Fermentation & Enzyme Technology, New York, J. Wiley & Sons, Acta Biotechnologica 0 (1980), 67-68. https://doi.org/10.1002/abio.370000013

[43] I. V. Tetko, P. Bruneau, Application of ALOGPS to predict 1-octanol/water distribution coefficients, logP, and logD, of AstraZeneca in-house database, Journal of Pharmaceutical Sciences. 93 (2004) 3103–3110. https://doi.org/10.1002/jps.20217.

[44] Lay. W, Zhang. J, Tang. C, Wang. R, Liu. Y, Fane. A, Analysis of Salt Accumulation in a Forward Osmosis System, Separation Science and Technology, (2012), 1837-1848, 47(13), https://doi.org/10.1080/01496395.2012.692423.

[45] Hancock. N, Cath. T, Solute coupled diffusion in osmotically driven membrane processes, Environmental Science and Technology, (2009), 6769-6775, 43(17), https://doi.org/10.1021/es901132x.

[46] C.Y. Tang, Q. She, W.C.L. Lay, R. Wang, A.G. Fane, Coupled effects of internal concentration polarization and fouling on flux behavior of forward osmosis membranes during humic acid filtration, Journal of Membrane Science. 354 (2010) 123–133. https://doi.org/10.1016/j.memsci.2010.02.059.

[47] J.R. McCutcheon, M. Elimelech, Influence of concentrative and dilutive internal concentration polarization on flux behavior in forward osmosis, Journal of Membrane Science. 284 (2006) 237–247. https://doi.org/10.1016/j.memsci.2006.07.049.

[48] S. Loeb, L. Titelman, E. Korngold, J. Freiman, Effect of porous support fabric on osmosis through a Loeb-Sourirajan type asymmetric membrane, 1997.

[49] V. Silva, V. Geraldes, A.M. Brites Alves, L. Palacio, P. Prádanos, A. Hernández, Multi-ionic nanofiltration of highly concentrated salt mixtures in the seawater range, Desalination. 277 (2011) 29–39. https://doi.org/10.1016/j.desal.2011.03.088.

[50] G.B. van den Berg, I.G. Racz, C.A. Smolders, Mass transfer coefficients in cross-flow ultrafiltration, Journal of Membrane Science, 47 (1989) 25-51, https://doi.org/10.1016/S0376-7388(00)80858-3

[51] A. Tiraferri, N.Y. Yip, A.P. Straub, S. Romero-Vargas Castrillon, M. Elimelech, A method for the simultaneous determination of transport and structural parameters of forward osmosis membranes, Journal of Membrane Science. 444 (2013) 523–538. https://doi.org/10.1016/j.memsci.2013.05.023.

[52] C. Bellona, J.E. Drewes, P. Xu, G. Amy, Factors affecting the rejection of organic solutes during NF/RO treatment - A literature review, Water Research. 38 (2004) 2795–2809. https://doi.org/10.1016/j.watres.2004.03.034.

[53] R. Online, L. Nghiem, A. Schaefer, M. Elimelech, Role of electrostatic interactions in the retention of pharmaceutically active contaminants by a loose nanofiltration membrane, Journal of Membrane Science, 286 (2006) 52-59. http://ro.uow.edu.au/engpapers/2642.

[54] Arizaa. M, Ctiasa. A, Malfeitob. J, Benaventea. J, Effect of pH on electrokinetic and electrochemical parameters of both sub-layers of composite polyamide/polysulfone membranes, Desalination 148 (2002), 377-382.

[55] S. Kim, K.H. Chu, Y.A.J. Al-Hamadani, C.M. Park, M. Jang, D.H. Kim, M. Yu, J. Heo, Y. Yoon, Removal of contaminants of emerging concern by membranes in water and wastewater: A review, Chemical Engineering Journal. 335 (2018) 896–914. https://doi.org/10.1016/j.cej.2017.11.044.

[56] Y. Gao, Z. Fang, P. Liang, X. Huang, Direct concentration of municipal sewage by forward osmosis and membrane fouling behavior, Bioresource Technology. 247 (2018) 730–735. https://doi.org/10.1016/j.biortech.2017.09.145.

[57] M. Xie, L.D. Nghiem, W.E. Price, M. Elimelech, Relating rejection of trace organic contaminants to membrane properties in forward osmosis: Measurements, modelling and implications, Water Research. 49 (2014) 265–274. https://doi.org/10.1016/j.watres.2013.11.031.

[58] Z. Wang, J. Tang, C. Zhu, Y. Dong, Q. Wang, Z. Wu, Chemical cleaning protocols for thin film composite (TFC) polyamide forward osmosis membranes used for municipal wastewater treatment, Journal of Membrane Science. 475 (2015) 184–192. https://doi.org/10.1016/j.memsci.2014.10.032.

[59] P. Prádanos, J.I. Arribas, A. Hernández, Mass transfer coefficient and retention of PEGs in low pressure cross-flow ultrafiltration through asymmetric membranes, 99 (1995) 1-20.

Figure Captions

Figure 7. Schematic illustration of the FO setup.

Figure 8. Maximum water flux, $J_{w,max}$ (left axis) and reverse salt flux, J_s (right axis) versus FS Flow rates.

Figure 9. Maximum water flux (left axis) and reverse salt flux (right axis) versus concentration of salt in the bulk of the DS.

Figure 10. Maximum Water Flux Values versus DS Osmotic Pressure in Bulk. The curve corresponds to the fit of the data to the model (Equation (5)).

Figure 11. Reverse saline flux versus maximum water flux.

Figure 6. Rejection of contaminants grouped according to their charge at pH=7.

Figure 7: Rejection according to the molecular weight and the hydrophobic/hydrophilic character of the permeating substances.

Figure 8. Recovery in the different stages.

Figure 9: Recovery in the FS of the different CECs after the rejection test against the molecular weight and log D.

Figure 10: Recovery of Atenolol after the rejection test and after several washings. Experiments have been made with different concentrations of atenolol in FS and with different concentrations of NaCl in DS.

Table Captions

Table 3. Specifications for the Aquaporin Inside ^{TM} FO hollow fiber module as provided by the membrane manufacturer.

Table 4. Properties of compounds**.**